

Article

Design Considerations of a Simplified Multiple Dividing Wall Column Pilot Plant

Ulrich Preißinger *, Lena-Marie Ränger and Thomas Grützner

Laboratory of Thermal Process Engineering, Institute of Chemical Engineering, Ulm University, 89081 Ulm, Germany; lena.raenger@uni-ulm.de (L.-M.R.); thomas.gruetzner@uni-ulm.de (T.G.)

* Correspondence: ulrich.preissingner@uni-ulm.de

Received: 22 February 2019; Accepted: 30 March 2019; Published: 3 April 2019



Abstract: This contribution elaborates the design considerations of a simplified version of a four-product multiple dividing wall column in pilot plant scale that will be built at Ulm University. This will be the first realization of a multiple dividing wall column worldwide. A detailed simulation approach, starting from the initialization by V_{min} -method, is presented to obtain a feasible design of the column, taking into account the constraints of the operation within a university environment. The operating point was found by simulation studies, using the integrated optimization tool of AspenPlus[®] V10. It is shown that an NQ-curve can be applied on simplified multiple dividing wall columns. Based on the determined operating point, the thermodynamic and the fluid dynamic design of the pilot plant are discussed in detail. It is shown that the designed column can be operated to obtain all products with a purity of at least 98 mol%.

Keywords: distillation; multiple dividing wall column; four product column; pilot plant design

1. Introduction

In the chemical industry, distillation is a wide spread and very energy consuming separation process and, therefore, the attempts to reduce the energy requirement are manifold. One very promising way to do this are dividing wall columns (DWC), which have become popular over the past 30 years, as they show savings in capital expenditures (CAPEX) and operational expenditures (OPEX) of around 30% [1–3]. As the industry has recognized the potential of DWCs, the number of installed applications is steadily increasing. In 2011, 125 DWCs were in operation [2], with the number likely to have increased rapidly due to revamps and new built applications. The DWC can be considered as a state-of-the-art technology nowadays [1–5]. Multiple dividing wall columns (mDWCs) with more than one partitioning wall are the consequent evolution of DWCs, since they offer the possibility to produce four or more pure product fractions in one column shell with further reduction of CAPEX and OPEX compared to classical sequences as the direct split. The mDWC with three partitioning walls (Figure 1a), also called the 2-3-4 configuration (two products from the prefractionator, three products from the middle fractionator, and four products from the main fractionator), can be operated in the thermodynamic optimum [6]. This means that it has the minimum energy requirement for the given separation task, as, in every separation section of the column, the easiest separation is always carried out. However, the complexity of this mDWC is increasing compared to DWCs with just one partitioning wall as the degrees of freedom are increasing from 12 to 23 [7]. This is the reason there is no evidence of a real mDWC plant in operation yet, at neither industrial nor laboratory scale. One opportunity to make an implementation more possible in the future is given by simplified four-product mDWCs, since they can be designed with fewer than three partitioning walls and are therefore easier to realize and operate. Figure 1b shows a simplification of a mDWC with the second wall in the upper part of the column, referred as the 2-2-4-a configuration. This simplification was already investigated by

different authors, since it can be operated with the same energy demand as the 2-3-4 configuration for some specific mixtures of industrial relevance [8–10]. Figure 2 shows other simplified versions of four-product DWCs. Figure 2a represents the Kaibel Column, a single-partitioned DWC with four product streams [11]. This column has the big advantage of a relatively simple constructional design, but it cannot be operated in the thermodynamic optimum. In Figure 2b, another simplified mDWC, which is very similar to the one in Figure 1b, with the second partitioning wall in the lower area, referred as the 2-2-4-b configuration, is depicted. Whether the 2-2-4-a configuration or the 2-2-4-b configuration is the better choice for a separation task is solely related to the properties of the feed mixture, since the constructional design effort is similar. The big advantage of simplified mDWCs is the reduction of design variables. This is due to the reduced number of partitioning walls, resulting in a reduced number of gas and liquid splits. Different research groups already investigated the potential of an industrial implementation of the 2-2-4-a configuration. A detailed dimensioning of a simplified mDWC with three partitioning walls and two overhead condensers was done by Dejanović et al. In addition, this publication compares five different column configurations of standard DWC and mDWCs, with 2-2-4-a configuration being the best solution [9]. In another work, Olujić et al. presented an approach of a detailed dimensioning of three different four-product columns. Their investigations on the Kaibel Column, the 2-3-4 configuration and the 2-2-4-a configuration show that the latter is the most suitable for a practical implementation [10].

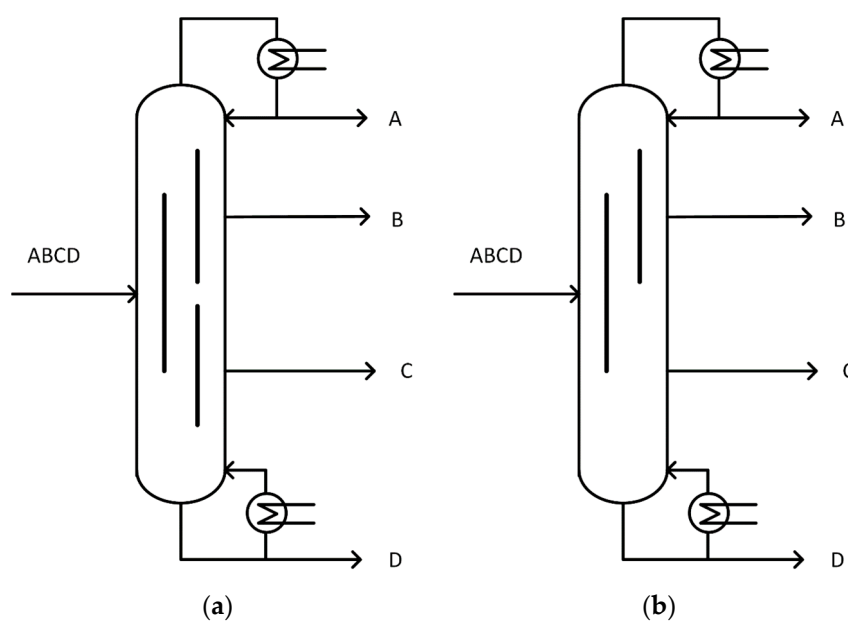


Figure 1. Configurations of multiple dividing wall columns: (a) 2-3-4 configuration with three partitioning walls; and (b) 2-2-4-a configuration with the additional wall in the upper area of the column.

For the operational performance of mDWCs, especially the internal gas and liquid splits are crucial. While it is possible to adjust the liquid split by using specifically designed liquid distributors, there is still no way to manipulate the gas split. A recent publication [12] proposes the application of special chimney trays for the direct manipulation of the vapor split. However, the industrial proof of feasibility for this type of equipment is still missing. Nevertheless, columns with two internal gas splits could not be investigated in practice yet. Therefore, it is difficult to make a prediction about the operational stability of such a column. Remedy can be provided by dynamic simulations, as they can be used for the investigation of control structures or the prediction of the dynamic behavior of the column. Lukač et al. presented two different promising control structures for the 2-2-4-a configuration. For controlling the column, mainly temperature measurements are being used. Their results show that using a temperature difference control for one product stream can respond well to fluctuations in

the feed stream composition [13]. Building a simplified mDWC offers the opportunity of answering questions in regards of the controllability, the behavior of two vapor splits in one column shell and the operation of a column with more than one partitioning wall in general.

This publication presents a structured way from the first idea to the design of the pilot plant in detail. Topics that are discussed in the following parts are the initialization of the simulation, the simulation model and how a promising operating point can be found, the thermodynamic and the fluid dynamic design as well as the sizing of the column.

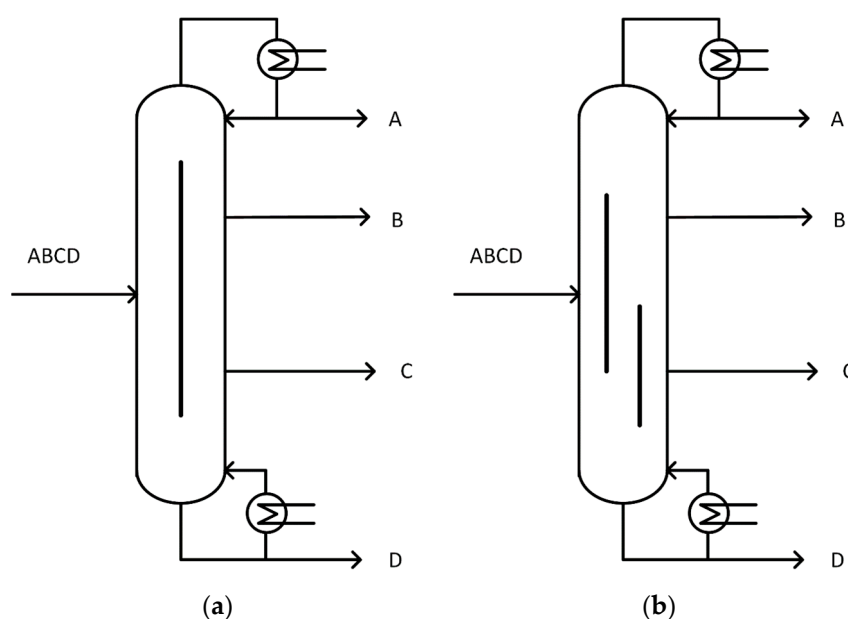


Figure 2. Simplifications of multiple dividing wall columns: (a) Kaibel Column with one partitioning wall; and (b) 2-2-4-b configuration with the additional wall in the lower area of the column.

2. Test Systems and Simulation Model

First, the question must be clarified if the 2-2-4-a configuration or the 2-2-4-b configuration is better suited for a pilot plant realization. Since the applicability of the two setups is determined mainly by the properties of the mixture, the first step was to define potential test systems for the column. Note that the column will be operated in a university environment. Therefore, there are strict constraints regarding toxicity, environmental impact, and fire hazard, as well as the price. For this purpose, a pool of components consisting of six different groups of substances was used to do a feasibility analysis with the main evaluation criteria toxicity, fire hazard and environmental compatibility. Further investigations, such as a price comparison of the components were carried out. In the next step, the Vapor–Liquid Equilibria (VLE) were investigated to prove if azeotropic behavior occurs in binary sub-systems. The physical property package of the process simulator AspenPlus[®] V10 was used for this purpose. The test systems applied in the column should strictly show zeotropic behavior. In the case that binary azeotropes occur, it is assured that these systems will not be present in the final mixtures. This resulted in seven different systems that can potentially be used in the mDWC. The pool of components and the resulting systems can be found in Table A1 in Appendix A. The next step was to check the energy requirement of the two configurations of simplified mDWCs for the chosen mixtures compared to the 2-3-4 configuration, which represents the energetic optimum. This step was carried out based on the V_{min} -diagram. Using V_{min} -diagrams for energetic evaluations is described in detail elsewhere [7,14]. Compared to the energetic optimum of the 2-3-4 configuration, all investigated systems within the 2-2-4-b configuration showed a higher energy demand and therefore an energy penalty. For the 2-2-4-a configuration, all investigated systems with the exception of one could be distilled without an energy penalty. This is System 2 in Table A2 (Appendix A). A subsequent

literature search also proved that the 2-2-4-a configuration is better suited for industrial applications, which is why the decision fell on this configuration [8,10,15].

Since commercial process simulators do not offer unit operation models for mDWCs, substitute models have to be applied here [5]. These are usually built up with thermally coupled simple distillation columns. The most common one is the extended Petlyuk scheme shown in Figure 3. This is the thermodynamically equivalent substitute model to the mDWC with three dividing walls that shows the minimum energy requirement for any given separation task [16]. Note that the columns, besides C31 and C33, do not have an evaporator or condenser.

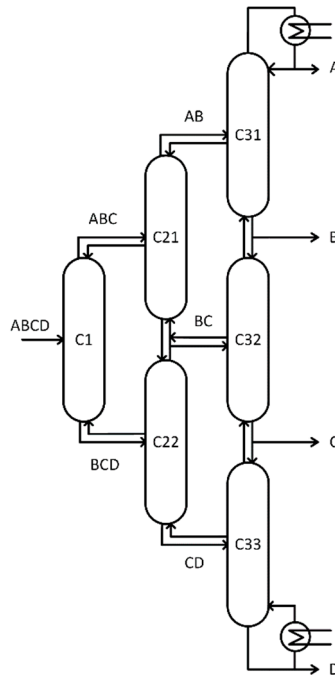


Figure 3. Depiction of the extended Petlyuk substitute model.

To represent the simplified mDWC configuration, the Petlyuk scheme has to be modified, in a way that the substitute model is thermodynamically equivalent to the 2-2-4-a configuration. The target was to build up the substitute model with the fewest unit operation models and the fewest recycle streams to facilitate the convergence within the simulation. Figure 4 shows how the resulting model was used in the simulator. To achieve convergence in the initial simulation, meaningful estimations have to be provided for all recycle streams. The estimated values were again found by the V_{min} -method. How simulations are robustly initialized by this method can be found elsewhere [7,14]. The thermodynamic model used in the simulation was non-random-two-liquid (NRTL), since it has a very good accuracy and is recommended for alcoholic mixtures, which were solely used in the simulation [17]. To model the columns within the AspenPlus[®] environment, the RadFrac model was used. The equilibrium stage model is absolutely sufficient for the needs of the desired studies. Since the V_{min} -method requests an infinite number of theoretical stages, the initialization of the rigorous substitute model was carried out consequently with an impractically large number of stages. Hence, the stages have to be reduced to a practical number in the next step.

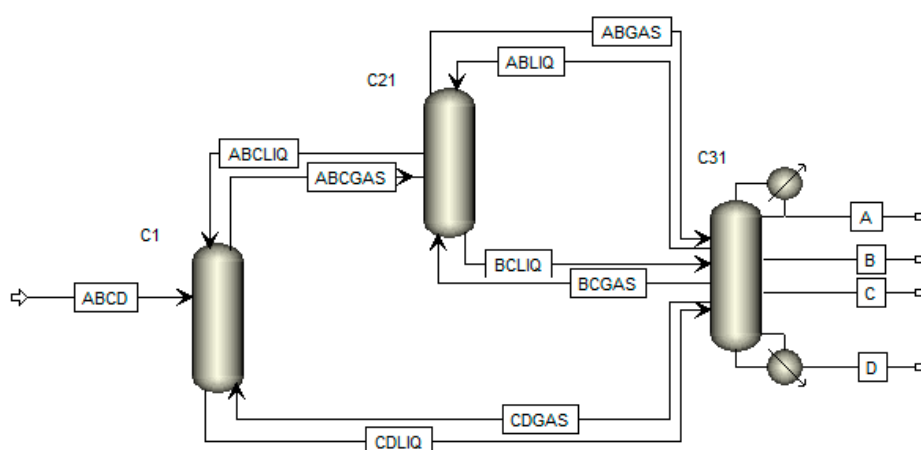


Figure 4. Simulation Model used in the process simulator AspenPlus[®] to simulate the pilot plant.

A practical heuristic approach to do this for simple DWCs was presented by Dejanović et al. The proposed approach is described for three-product DWCs. To apply it to four-product mDWCs, some adaptations have to be done. The approach of Dejanović et al. starts the simulation with many stages, i.e. four times the minimum number of stages, calculated by the Fenske equation. Then, the vapor and liquid splits are optimized and the reboiler duty is minimized by using the optimization tool built in ChemCAD[®]. This step is repeated, while the number of stages is gradually reduced to a practical number of stages [18]. To apply this approach to simplified mDWCs, it is important to note that now two gas and liquid splits have to be optimized, while the number of stages is reduced. That means that four different independent variables are used to minimize the objective function (reboiler duty), while the number of stages in each section of the column are gradually and manually reduced. In this work, the optimization tool provided by AspenPlus[®] was used.

The determination of the operating point is illustrated by an example. For this purpose, the procedure of Dejanović et al. was used and the necessary adjustments were made to transfer this procedure to four-product mDWCs. The properties of the feed stream used in this example are shown in Table 1. To ensure that the thermodynamic model was appropriate and thus the simulation results were correct, all binary VLE were first checked using literature data from the Dortmundur Datenbank (DDB). Four components resulted in six binary VLE that have to be checked. The VLE representation of NRTL was in good accordance with the literature data and could be used without further adaptations.

Table 1. Feed stream properties and conditions used for the simulation.

Parameter	Value	Unit
Mole flow	0.1	kmol/h
Temperature	96.0	°C
Pressure	1	bar
Liquid Fraction	1	1
Ethanol	25	mol%
Propanol	25	mol%
Isobutanol	25	mol%
Butanol	25	mol%

To create the V_{min} -diagram, the relative volatilities were necessary. These were obtained by reading out the K-values from Aspen HYSYS[®] V10 and dividing them by the K-value of the heavy boiler, resulting in α_i [4.7, 2.2, 1.5, 1]. Aspen HYSYS[®] was used here, because in contrast to AspenPlus[®] this simulator allows reading out the K-values directly from the feed stream. The resulting V_{min} -Diagrams for the 2-3-4 configuration and 2-2-4-a configuration are shown in Figure 5. Note that there was no energy penalty for this system, since the CD split remained the highest point in the diagram. From

this diagram, the necessary information for the initialization of the above-mentioned substitute model was obtained.

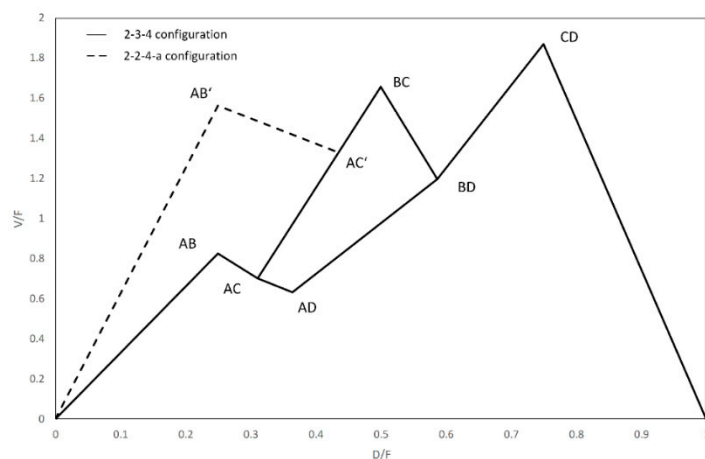


Figure 5. V_{min} -diagram of a quaternary feed mixture containing: Ethanol (A); Propanol (B); Isobutanol (C); and Butanol (D) ($z_i = 0.25$; $q = 1$). Dashed lines indicate the increased energy demand for the sharp AB' and AC' split within the 2-2-4-a configuration, which does not result in an energy penalty, since the highest peak remains the sharp split CD.

To start the simulation, many theoretical stages were provided to approximate an infinite number of stages, as assumed by the V_{min} -method. Fifty stages per separation section were chosen here. The initial values to start-up the simulation are shown in Table 2. The parameter Quality A, for example, represents the purity of Component A in the stream in which this component occurs most. In the case of Component A, this is the distillate stream. The same applies for the other product qualities in this table. For clarification, the parameters in Table 2 are referenced in Figure 6. Note that the section C_1^B possessed twice the theoretical stages as all other sections. The reason is explained in Section 3. The empty lines in the initial value column of Table 2 are the results of the converged simulation and no values were necessary for the initialization of the simulation.

Table 2. Initial values for the simulation and results of the initialization and the first optimization step.

Parameter	Initial Values	After Initialization	50 Number of Stages	Unit
Stages in all sections	50	50	50	1
Stages C_1^B	100	100	100	1
Reboiler duty		1.98	2.28	kW
Reflux rate		0.16	0.19	kmol/h
Boilup rate	0.17	0.17	0.19	kmol/h
LSplit1 left	0.09	0.09	0.11	kmol/h
LSplit1 right		0.06	0.07	kmol/h
LSplit2 left	0.06	0.06	0.07	kmol/h
LSplit2 right		0.03	0.03	kmol/h
VSplit1 left	0.01	0.01	0.01	kmol/h
VSplit1 right		0.05	0.05	kmol/h
VSplit2 left	0.12	0.12	0.14	kmol/h
VSplit2 right		0.06	0.07	kmol/h
Quality A		97.7	98.8	mol-%
Quality B		95.1	98.3	mol-%
Quality C		88.3	98.0	mol-%
Quality D		90.7	98.5	mol-%

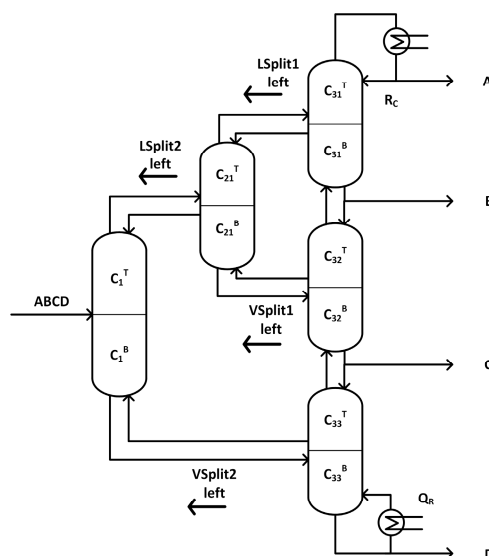


Figure 6. Thermodynamic equivalent substitute model for 2-2-4-a configuration, which contains all important parameters.

The results obtained after converged initialization are also shown in Table 2. Since the product purity after initialization was very poor, it should be mentioned at this point that the V_{min} -method was based on assumptions, such as constant internal molar flows and an infinite number of stages, which no longer held in the presented simulation. Based on this convergent simulation, the AspenPlus[®] optimization tool was used to obtain an optimized operating point that meets all given boundary conditions. The boundary conditions were product purities of at least 98 mol-% of the major component in the respective stream. To achieve this, the internal gas and liquid splits were used as independent variables, while the objective function, the reboiler duty, was minimized. Because optimizers generally have problems solving too many different variables, it might be possible to obtain a solution of a local minimum instead of the global minimum. This is due to poorly chosen starting values. To avoid this problem, different starting points were used within the optimization. The best value was then taken as the result. The operating point after applying the optimization for 50 stages in every section is shown in Table 2. Now, all product specifications could be fulfilled, but as expected the reboiler duty increased from 1.98 kW to 2.28 kW. In other words, the minimum energy demand of the V_{min} -diagram cannot be achieved in real operation. Since a practical number of stages is mandatory, the energy demand inevitably increases.

The next step was to reduce the number of stages in all sections and repeat the procedure with the optimization tool. Since the same packings with the same height were installed in all sections, the number of stages in all sections was uniformly reduced. This was conducive to the purpose of keeping the pressure loss equal on both sides of the partitioning walls, which is further discussed in Section 3. The results of the stepwise minimization of the number of stages are shown in Table 3. It can be seen that the reboiler duty increased with decreasing number of stages. This result is expected, since more energy is necessary to separate the four components with a lower number of stages.

The results in Table 3 can be understood as a NQ-curve for the 2-2-4-a configuration of a mDWC. Note that a NQ-curve is only valid for one specific product purity for the case that all design parameters are optimized. As shown in Table 3, the results for the product quality vary in a small range due to the chosen optimization procedure. Strictly speaking, the operating points in Table 3 are not located on the same NQ-curve. Rather, the points listed there are overlaps of different NQ-curves resulting from the varying product composition. Nevertheless, connecting all points by interpolating the progression in between resulted in the typical shape of a NQ-curve. The NQ-curve shown in Figure 7 represents the NQ-curve for the product quality of component C being 98 mol%. Included in this diagram are

the extreme compromises between the number of stages and the energy demand, represented by the value for the minimum reboiler duty, shown as the highest point in the diagram and the value for the minimum number of stages, shown as the lowest point in the diagram. The number of stages for these two points are 50 stages per section (overall stage number: 550) and 13 stages per section (overall stage number: 143), respectively. The operating point was determined in the area of the greatest curvature, since this is the best compromise between the number of stages and the reboiler duty. This is the final design point of the column.

Table 3. Results of the stepwise reduction of the number of stages in all sections.

Parameter	40 Stages	30 Stages	20 Stages	15 Stages	13 Stages	Unit
Stages in all sections	40	30	20	15	13	1
Stages C_1^B	80	60	40	30	26	1
Reboiler duty	2.29	2.37	3.21	6.18	19.1	kW
Reflux rate	0.19	0.19	0.27	0.54	1.73	kmol/h
Boilup rate	0.19	0.20	0.27	0.52	1.60	kmol/h
LSplit1 left	0.13	0.13	0.13	0.34	0.14	kmol/h
LSplit1 right	0.05	0.06	0.14	0.21	1.50	kmol/h
LSplit2 left	0.07	0.07	0.07	0.17	0.07	kmol/h
LSplit2 right	0.06	0.06	0.06	0.15	0.06	kmol/h
VSplit1 left	0.05	0.04	0.04	0.13	0.05	kmol/h
VSplit1 right	0.03	0.04	0.11	0.19	1.54	kmol/h
VSplit2 left	0.13	0.13	0.13	0.22	0.13	kmol/h
VSplit2 right	0.07	0.08	0.16	0.33	1.69	kmol/h
Quality A	99.4	100.0	100.0	100.0	100.0	mol-%
Quality B	99.1	99.6	98.8	99.2	99.2	mol-%
Quality C	98.0	98.0	98.0	98.0	98.0	mol-%
Quality D	98.2	98.4	99.2	98.8	98.7	mol-%

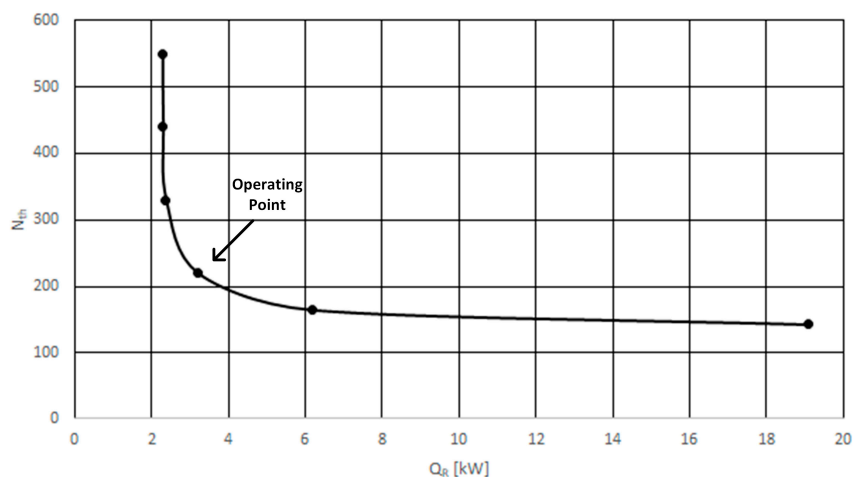


Figure 7. NQ-curve with interpolated spline of the simulation results with product purities of at least 98 mol%.

3. Design of the Pilot Plant

The thermodynamic design from mDWCs (leading to the number of stages and, hence, the internal streams for that specific case) is typically separated from the fluid dynamic design (leading to the areas of the column sections). First, the thermodynamic design is carried out, since it contains the information about the number of stages, as well as the gas and liquid loads in each section. Subsequently, the fluid dynamic design is performed. The thermodynamic design of the column has already been done with the selection of the operating point (see Section 2). Figure 8 shows the internal gas and liquid flows at the top and bottom of each section for the chosen operating point and the feed

stream shown in Table 1. In addition, the reflux ratio (denoted as L/D) and the boil up ratio (denoted as V/B), as well as the number of stages in each section are illustrated. Since the feed stream and the side streams are liquid streams, they only influence the liquid load in the column.

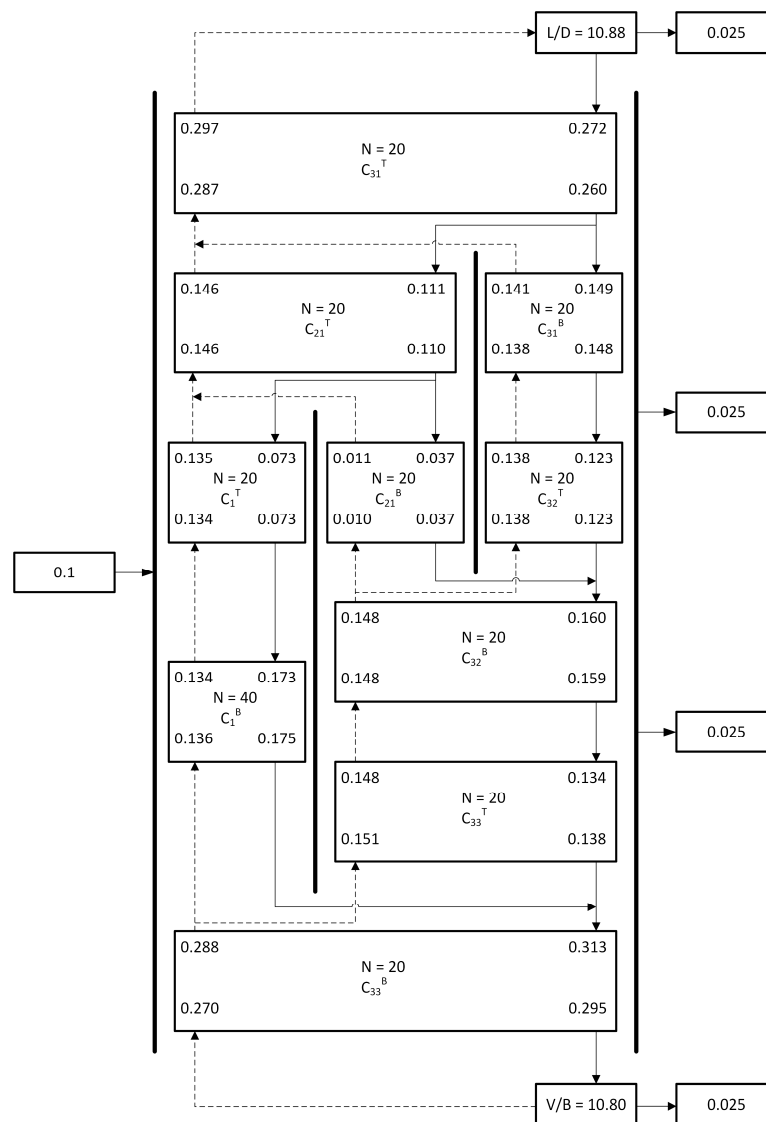


Figure 8. Internal gas and liquid loads at the top and bottom of all sections of the pilot plant. The solid lines represent the liquid flow and the dashed lines the gas flow in kmol/h.

Within the fluid dynamic design, the area of each section of the columns has to be determined to realize meaningful loads of vapor and liquid. For this purpose, the internal gas flows obtained from the thermodynamic design are used. The F -Factor was used as a decision criterion to choose the correct diameters, as it is easy to calculate.

$$F = u_G \times \sqrt{\rho_G} \quad (1)$$

For laboratory packings, usually the F -Factor should be less than 1. To keep the column flexible, it was decided to go for rather larger diameters for the column sections. This also has positive effects on the heat loss and provides flexibility for future, unknown, separation tasks. Since the mDWC will be realized in a Brugma configuration where all column sections are single shells, a circular cross sectional area can be assumed. The features of the column are further discussed in Section 4. The chosen diameters is shown in Table 4. The starting point of our deliberations was to use only a

small number of different diameters. This was again to maintain the high degree of flexibility of the plant. The associated F -Factors are shown in Figure 9a. It reveals a very small F -Factor in the column section C_{21}^B , while all other sections can load well. However, these are the F -Factors obtained from the gas loads of the operating point as determined from the thermodynamic design. From the selection of the section diameters, it becomes clear that the sides of the partitioning walls will have equal cross sectional areas. Moreover, the sections are packed with the same structured packings of the same height. Hence, the pressure loss of the sections is equal and the gas will uniformly split in a 1 to 1 ratio. As a result, the vapor distribution is forced to change due to constructive constraints and can neither be manipulated nor maintained at the original design values. In the next step, the achieved operating point was adjusted, taking the resulting vapor split into account.

Table 4. Diameters in the respective column section.

Column Section	Diameter	Unit
C_1^T	50	mm
C_1^B	50	mm
C_{21}^T	50	mm
C_{21}^B	50	mm
C_{31}^T	80	mm
C_{31}^B	50	mm
C_{32}^T	50	mm
C_{32}^B	50	mm
C_{33}^T	50	mm
C_{33}^B	80	mm

Starting from the design case, the vapor splits were adjusted until the same average F -Factors on both sides of the partitioning walls were achieved to make sure that the gas distributes evenly. Note that an additional section was needed in the area C_1^B to keep the pressure drop on both sides of the partitioning walls equal. In this particular case, this meant 60 theoretical stages on the left side of the partitioning wall (C_1^T and C_1^B) and 60 stages on the right side (20 in C_{21}^B , 20 in C_{32}^B and 20 in C_{33}^T). To find the real gas distribution, the procedure was as follows. First, VSplit2 was set to have an equal F -Factor on both sides of the partitioning walls. Afterwards, VSplit1 was adjusted, since it depended on VSplit2. When the equal F -Factors on both sides of the partitioning walls were set, the optimization tool was used to optimize the liquid splits, while reducing the objective function, the reboiler duty. To ensure that the gas was still distributed evenly, this procedure must be repeated until the minimum reboiler duty was found, while all constraints were still fulfilled. The starting F -Factors in each section for this procedure are shown in Figure 9a, while the final F -Factors in each section are shown in Figure 9b. The values for the internal splits and the product purities are shown in Table 5. It is noticeable here that the reboiler duty of the adapted gas distribution was now lower and beneath the original value. This is because another operating point with different product specifications was found. The new operating point caused a lower reboiler duty, because the product purity of Component B increased while Component D decreased and, as the V_{min} -diagram in Figure 5 shows, it was easier to separate Component B from Component C in this mixture than Component C from Component D. It was thus demonstrated that an operating point with the product specifications of at least 98 mol% in every product stream of the column designed in this contribution can be achieved for the given system. Not shown here, but proved, was also the applicability of the other mentioned test systems in the provided column setup. This results from an investigation of the different V_{min} -diagrams of all mixtures. Since the mixture chosen for designing the column was the most difficult one to separate, it can be assumed that all other mixtures could be separated in the same column with the same utilities.

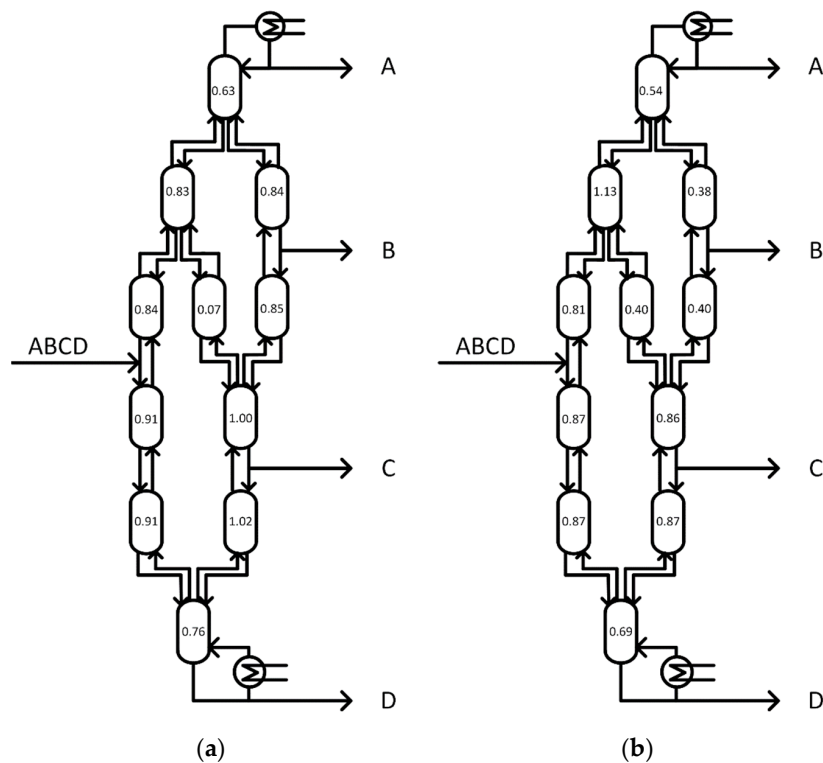


Figure 9. Depiction of a substitute model of the pilot plant: (a) including the F -Factors in each section obtained by the optimized operating point starting from the V_{min} -method; and (b) real F -Factor distribution.

Table 5. Comparison of the adapted gas distribution to the operating point of the thermodynamic design.

Parameter	Operating Point	Adapted Gas Distribution Reduced Reboiler Duty	Unit
Stages in all sections	20	20	1
Stages C_1^B	40	40	1
Reboiler duty	3.21	2.92	kW
Reflux rate	0.27	0.24	kmol/h
Boilup rate	0.27	0.24	kmol/h
LSplit1 left	0.13	0.15	kmol/h
LSplit1 right	0.14	0.09	kmol/h
LSplit2 left	0.07	0.07	kmol/h
LSplit2 right	0.06	0.07	kmol/h
VSplit1 left	0.04	0.06	kmol/h
VSplit1 right	0.11	0.06	kmol/h
VSplit2 left	0.13	0.13	kmol/h
VSplit2 right	0.16	0.13	kmol/h
Quality A	100.0	100.0	mol-%
Quality B	98.8	99.2	mol-%
Quality C	98.0	98.0	mol-%
Quality D	99.2	98.8	mol-%

4. Design Features of the Pilot Plant

To build the pilot plant column, the Brugma configuration was chosen, as it is easy to construct and heat transfer across the partitioning walls is eliminated. In addition, it is a proven setup for DWCs with only one partitioning wall [19]. Figure 10 shows the setup of the column. In the Brugma configuration, each separation section is carried out as a separate column and the pilot plant thus does not consist of a single column shell with two partitioning walls but of several thermally coupled

simple columns. Since the column should be built in the laboratory facilities of Ulm University, there is a limitation given in the height of the column of 10 m. The height of the column is mainly determined by the number of stages in the main fractionator. The main fractionator consists of sections C_{31}^T , C_{31}^B , C_{32}^T , C_{32}^B , C_{33}^T and C_{33}^B . To accomplish 20 stages per section, it was decided to choose the Montz-Pak A3-1000, since this packing has more than 20 stages per meter at an F -Factor of less than one (see Figure A1 in Appendix B). Each packing is around 1 m long and the main fractionator consists of six different separation sections. Additionally, the two side draws for the product streams as well as the two internal liquid splits are equipped with shaking funnels. Considering the connecting parts for the gas and liquid splits as well as the height of the reboiler and condenser, the pilot plant reaches a height of 9.8 m, thus remaining lower than the limitation of 10 m.

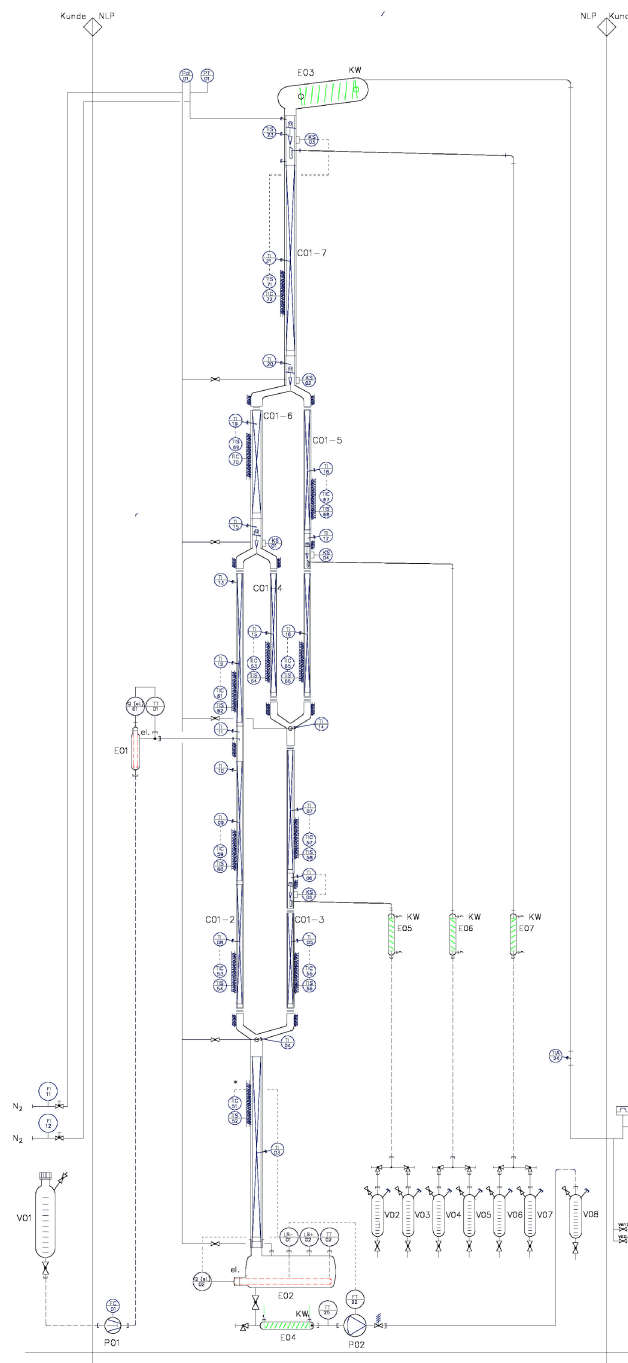


Figure 10. P&ID of the pilot plant [20].

All column shells in this configuration are made of glass. The feed tank is connected via the feed pump, that can be operated with a flow rate of 0–10 L/h, with the pre-fractionation section of the column. To feed boiling liquid to the column, an electrical feed preheater with a duty of 0.7 kW is installed. The column is equipped with a water cooled condenser in the top and an electric kettle evaporator, providing a duty of 5 kW, in the bottom. In addition, all product streams are cooled by water condensers. First, the column will be operated at atmospheric pressure, with the possibility of implementing a vacuum pump later for the operation in sub-atmospheric pressure. To be able to evacuate the product tanks individually during the operation, they are accomplished redundantly. With the purpose of avoiding heat loss, double-walled, evacuated shells with heating sleeves are used. The column shells are implemented modularly and can easily be exchanged by other column shells with the same height.

To control the column most flexibly, the following control possibilities are available. The distillate flow rate can directly be influenced by the shaking funnel, or can be controlled by a temperature measurement in the section C_{31}^T . With the purpose of measuring the temperature profile over the column appropriately and therefore to use these measurements for control issues, PT-100 temperature sensors are installed every 25 cm in the area of the packings. In addition, the side withdrawals as well as the internal liquid distributors can be controlled directly or by a temperature measurement. A pump controls the liquid level of the sump of the column. The evaporator is either controlled by the differential pressure over the entire column or by a temperature measurement in the section C_{33}^B . All proposed control possibilities offer a high flexibility as different control structures can be tested in the column. That also ensures that different test systems can be operated with different control structures and thus be separated in the pilot plant properly.

5. Conclusions

DWCs offer a great opportunity for saving both, energy and capital cost and are nowadays widely spread in the chemical industry. The consequent evolution of this application leads to four-product mDWCs, which increase the expected savings further. Unfortunately, the complexity of these plants is very high and, therefore, to the knowledge of the authors, no plant is in operation, neither in industry nor in academia. The laboratory of thermal process engineering at Ulm University aims to setup and operate a mDWC. To reduce the complexity, a simplified version of a mDWC is favored. It turned out that, for most of the considered mixtures, a configuration with two instead of three partitioning walls can be operated without an energy penalty. This is in accordance with the findings of other authors. The final design was carried out based on thermodynamic consistent substitute models. The V_{min} -method is in this context a powerful tool for fast and robust initialization of the rigorous column model. The final design of the column has to obey the constraints of the laboratory facility, mainly the building height. Therefore, the number of stages of the column has to be set to a practical value. This reduction was carried out in a structured way by means of the built-in optimization tool of AspenPlus[®] and a NQ-curve was extracted. By this procedure, it turned out that the optimizer is weak for such complex tasks and ending up in local minima could not always be avoided. Hence, the group is currently working together with the Fraunhofer Institute for Manufacturing Technology and Advanced Materials (IFMA) on a more powerful and reliable optimizer for solving mixed integer nonlinear programming (MINLP) problems. The final column is discussed in detail. We placed greatest emphasis on the flexibility of the plant. Different control structures can be applied. The used packing is not a dedicated laboratory packing, which facilitates the transferability of the results to industrial applications as well as offers a high number of theoretical stages per meter.

Author Contributions: U.P.: Methodology, Software, formal analysis, investigation, visualization, and writing—original draft. L.-M.R.: Validation and writing—review and editing. T.G.: Conceptualization, supervision, project administration, resources, and writing—review and editing.

Funding: This research received funding from “Deutsche Bundesstiftung Umwelt (DBU), Az 34815/01.

Acknowledgments: The authors gratefully acknowledge the valuable input of Dr. Matthias Stumpf (Normag Labor- und Prozesstechnik GmbH).

Conflicts of Interest: The authors declare no conflict of interest.

Symbols

B	Molar bottom stream	kmol/h
C	Column	1
D	Molar distillate stream	kmol/h
F	F -Factor	Pa ^{0.5}
L	Molar liquid flow	kmol/h
N	Number of Stages	1
Q_R	Reboiler duty	kW
q	Liquid fraction	1
R_c	Reflux rate	kmol/h
u	Superficial velocity	m/s
V	Molar vapor flow	kmol/h
z_i	Molar fraction of component i in the feed	mol/mol
ρ	Density	kg/m ³

Subscripts

G	Gas Flow
i	Component i
min	Minimum
th	theoretical

Superscripts

B	Bottom of column
T	Top of column

Abbreviations

CAPEX	Capital Expenditures
DDB	Dortmunder Datenbank
DWC	Dividing Wall Column
Liq	Liquid
mDWC	Multiple Dividing Wall Column
NRTL	Non-Random Two Liquid
OPEX	Operational Expenditures
VLE	Vapor–Liquid Equilibrium
LSplit1 left	Topmost liquid split to the left
LSplit1 right	Topmost liquid split to the right
LSplit2 left	Subsequent liquid split to the left
LSplit2 right	Subsequent liquid split to the right
VSplit1 left	Subsequent vapor split to the left
VSplit1 right	Subsequent vapor split to the right
Vsplit2 left	Bottommost vapor split to the left
VSplit2 right	Bottommost vapor split to the right

Appendix A

Table A1. Pool of components.

Component	Substance Group	CAS-NR
Ethanol	Alcohol	64-17-5
1-Propanol	Alcohol	71-23-8
Isobutanol	Alcohol	78-83-1
1-Butanol	Alcohol	71-36-3
Acetone	Ketone	67-64-1
Butanone	Ketone	78-93-3
3-M-Butanone	Ketone	563-80-4
2-Pentanone	Ketone	107-87-9
Hexanone	Ketone	591-78-6
Propanal	Aldehyde	123-38-6
Butanal	Aldehyde	123-72-8
Pentanal	Aldehyde	110-62-3
Hexanal	Aldehyde	66-25-1
Ethyl-Propyl-Ether	Ether	628-32-0
Di-n-Propylether	Ether	111-43-3
n-Hexane	Alkane	110-54-3
n-Heptane	Alkane	142-82-5
n-Octane	Alkane	111-65-9
Methyl acetate	Ester	79-20-9
Ethyl acetate	Ester	141-78-6
Propyl acetate	Ester	109-60-4
Butyl acetate	Ester	123-86-4

Table A2. Potential component systems.

System	Components
1	Methyl acetate Butanal Propanol Isobutanol
2	Methyl acetate Butanal Propanol Butanol
3	Methyl acetate Butanal Propyl acetate Butanol
4	Methyl acetate Butanal Isobutanol Butanol
5	Methyl acetate Propanol Isobutanol Butanol
6	Butanal Propanol Isobutanol Butanol
7	Ethanol Propanol Isobutanol Butanol

Appendix B

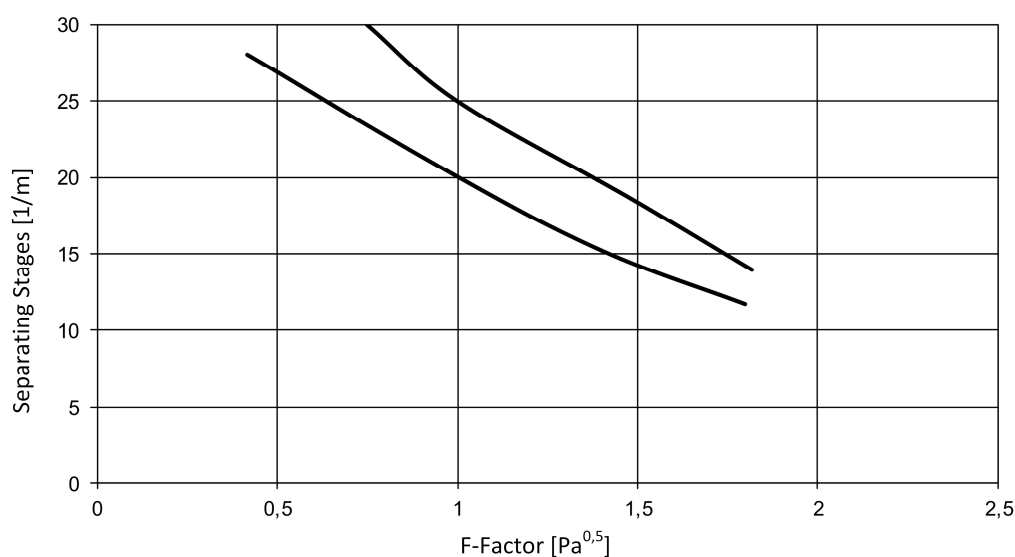


Figure A1. Separating stages plotted above the F -Factor for Montz-Pak A3-1000 for the test system Chlorobenzene/Ethylbenzene [21].

References

- Asprion, N.; Kaibel, G. Dividing wall columns: Fundamentals and recent advances. *Chem. Eng. Process. Process Intensif.* **2010**, *49*, 139–146. [[CrossRef](#)]
- Yildirim, Ö.; Kiss, A.A.; Kenig, E.Y. Dividing wall columns in chemical process industry: A review on current activities. *Sep. Purif. Technol.* **2011**, *80*, 403–417. [[CrossRef](#)]
- Dejanović, I.; Matijašević, L.; Olujić, Ž. Dividing wall column—A breakthrough towards sustainable distilling. *Chem. Eng. Process. Process Intensif.* **2010**, *49*, 559–580. [[CrossRef](#)]
- Staak, D.; Grützner, T. Process integration by application of an extractive dividing-wall column: An industrial case study. *Chem. Eng. Res. Des.* **2017**, *123*, 120–129. [[CrossRef](#)]
- Staak, D.; Grützner, T.; Schwegler, B.; Roederer, D. Dividing wall column for industrial multi purpose use. *Chem. Eng. Process. Process Intensif.* **2014**, *75*, 48–57. [[CrossRef](#)]
- Halvorsen, I.J.; Skogestad, S. Minimum Energy Consumption in Multicomponent Distillation. 3. More Than Three Products and Generalized Petlyuk Arrangements. *Ind. Eng. Chem. Res.* **2003**, *42*, 616–629. [[CrossRef](#)]
- Ränger, L.-M.; Preißinger, U.; Grützner, T. Multiple Dividing-Wall Columns—Current Status and Future Prospects. *Chem. Ing. Tech.* **2018**. [[CrossRef](#)]
- Halvorsen, I.J.; Dejanović, I.; Skogestad, S.; Olujić, Ž. Internal configurations for a multi-product dividing wall column. *Chem. Eng. Res. Des.* **2013**, *91*, 1954–1965. [[CrossRef](#)]
- Dejanović, I.; Halvorsen, I.J.; Skogestad, S.; Jansen, H.; Olujić, Ž. Hydraulic design, technical challenges and comparison of alternative configurations of a four-product dividing wall column. *Chem. Eng. Process. Process Intensif.* **2014**, *84*, 71–81. [[CrossRef](#)]
- Olujić, Ž.; Dejanović, I.; Kaibel, B.; Jansen, H. Dimensioning Multipartition Dividing Wall Columns. *Chem. Eng. Technol.* **2012**, *35*, 1392–1404. [[CrossRef](#)]
- Kaibel, G. Distillation columns with vertical partitions. *Chem. Eng. Technol.* **1987**, *10*, 92–98. [[CrossRef](#)]
- Kang, K.J.; Harvianto, G.R.; Lee, M. Hydraulic Driven Active Vapor Distributor for Enhancing Operability of a Dividing Wall Column. *Ind. Eng. Chem. Res.* **2017**, *56*, 6493–6498. [[CrossRef](#)]
- Lukač, G.; Halvorsen, I.J.; Olujić, Z.; Dejanović, I. On Controllability of Four-Product Dividing Wall Columns. *Chem. Eng. Trans.* **2018**, *69*, 259–264. [[CrossRef](#)]
- Ränger, L.-M.; Preißinger, U.; Grützner, T. Robust Initialization of Rigorous Process Simulations of Multiple Dividing Wall Columns via V_{min} Diagrams. *ChemEngineering* **2018**, *2*, 25. [[CrossRef](#)]

15. Jansen, H.; Dejanović, I.; Rietfort, T.; Olujić, Ž. Dividing Wall Column as Energy Saving Retrofit Technology. *Chem. Ing. Tech.* **2016**, *88*, 200–207. [[CrossRef](#)]
16. Petlyuk, F.B.; Platonov, V.M.; Slavinskii, D.M. Thermodynamically Optimal Method for Separating Multicomponent Mixtures. *Am. Inst. Chem. Eng. Int. Chem. Eng. A Q. J. Transl. Russ. East. Eur. Asia* **1965**, *5*, 555–561.
17. Valderrama, J.O.; Faúndez, C.A.; Toselli, L.A. Advances on modeling and simulation of alcoholic distillation. Part 1: Thermodynamic modeling. *Food Bioprod. Process.* **2012**, *90*, 819–831. [[CrossRef](#)]
18. Dejanović, I.; Matijašević, L.; Olujić, Ž. An Effective Method for Establishing the Stage and Reflux Requirement of Three-product Dividing Wall Columns. *Chem. Biochem. Eng. Q.* **2011**, 147–157.
19. Dwivedi, D.; Strandberg, J.P.; Halvorsen, I.J.; Skogestad, S. Steady State and Dynamic Operation of Four-Product Dividing-Wall (Kaibel) Columns: Experimental Verification. *Ind. Eng. Chem. Res.* **2012**, *51*, 15696–15709. [[CrossRef](#)]
20. Stumpf, M. *Multiple Dividing Wall Column Pilot Plant*; Normag Labor- und Prozesstechnik GmbH: Hofheim, Germany, 2019.
21. Julius Montz GmbH. *MONTZ-Pilotanlagen*; Julius Montz GmbH: Hilden, Germany, 2019.



© 2019 by the authors. Licensee MDPI, Basel, Switzerland. This article is an open access article distributed under the terms and conditions of the Creative Commons Attribution (CC BY) license (<http://creativecommons.org/licenses/by/4.0/>).